ELSEVIER

Hearing Research 79 (1994) 183–189

HEARING RESEARCH

Dynamic changes in tuning in the gerbil cochlea

Edwin R. Lewis [a,*], Kenneth R. Henry [b]

[a] *Department of EECS, University of California, Berkeley, CA 94720, USA*
[b] *Department of Psychology, University of California, Davis, CA 95616, USA*

Received 28 February 1994; revision received 6 June 1994; accepted 8 June 1994

Abstract

Afferent axons of the gerbil cochlear nerve were studied with reverse correlation analyses carried out with movable time windows and with noise that was modulated with a 10-Hz trapezoidal envelope that switched the noise amplitude between two levels, 20 dB apart. At the time of switching, the attributes of the axonal tuning curves derived in this manner switched very rapidly (e.g., within 10 ms) from those characteristic of lower-level stimuli to those characteristic of higher-level stimuli and vice versa. As previous investigators have shown, the attributes of tuning curves at higher levels include broader bandwidth and an accentuated low-frequency hump. Characteristic frequencies (CFs) of gerbil axons used in this study ranged from approximately 500 Hz to approximately 5 kHz. Over this range, the low-frequency hump was most pronounced in our studies for units with higher CFs, each of which showed a sharp high-frequency peak and a distinctly separate, broad low-frequency hump (reminiscent of the tip and tail of a conventional frequency-threshold tuning curve). The amplitude of the peak relative to that of the hump, and the breadth of the peak, both changed rapidly and reversibly following sudden change of noise level. Observation of such rapid changes of tuning would be difficult to achieve with conventional frequency-threshold tuning curves, derived from tonal stimuli.

Key words: Reverse correlation; Tuning; Cochlea

1. Introduction

Using noise stimuli and cross-correlation analyses, several investigators have found similar changes in the tuning of individual auditory nerve fibers as the rms stimulus amplitude was varied (Evans, 1977; Møller, 1977, 1978, 1986; Carney and Yin, 1988). The temporal waveform [crosscovariance function or reverse-correlation (REVCOR) function] derived from the analysis often is taken to be an estimate of the cochlear filter impulse response (de Boer and Kuyper, 1968; de Boer and de Jongh, 1978; Eggermont et al., 1983). As the noise stimulus amplitude is increased, this waveform appears to reflect increased damping; and its discrete Fourier transform (DFT) shows increased bandwidth. One investigator (Møller) also found that a hump appeared in the low-frequency region of the DFTs for some axons as the stimulus intensity was increased. The study that we report here was designed to investigate time courses of these various changes following abrupt changes in stimulus intensity. The stimulus was continuous noise with its intensity alternating up and down in 20-dB steps as a consequence of periodic modulation by a trapezoidal envelope (1.0 ms rise and fall times). REVCOR analysis was carried out over selected segments of the envelope period. We observed the same sorts of changes that were reported by the earlier authors, including the hump seen in Møller's DFTs for higher-level stimuli. In most instances, both for increases and decreases of stimulus amplitude, the changes clearly were completed well within the nominal duration of the REVCOR response waveform (including latency), typically a total of 3 to 10 ms.

2. Methods

Twenty seven axons from four animals were studied. The gerbil preparation used in this project was the same as that described in previous papers (e.g., Lewis and Henry, 1989). The bulla was opened and the

* Corresponding author. Fax: (510) 643 6103.

0378-5955/94/$07.00 © 1994 Elsevier Science B.V. All rights reserved
SSDI 0378-5955(94)00108-3

auditory nerve was exposed under the floor of the round-window antrum. Each axon studied was impaled by a glass micropipette electrode, filled with 3.0 M NaCl and having resistance greater than 50 MΩ. Auditory stimuli were applied through a closed-field system comprising an Etymotic ER-2 driver and a Etymotic ER-10 low-noise microphone sealed to the external auditory canal. Auditory axons were identified by their response to periodic noise bursts. Tone bursts were used to estimate best frequency and threshold at estimated best frequency. A tone burst at estimated best frequency and having a fast rise time was used to estimate response latency. Units were identified as being primary afferents by virtue of their response latencies (less than 2.0 ms), depth at penetration (less than 500 μm from the surface), and primary-like response to tone bursts at best frequency. The integrity of the cochlea and the general physiological condition of the animal subject were evaluated periodically by observing the threshold for compound action potential (obtained from a silver electrode placed in the niche of the oval window), in response to an 8-kHz stimulus.

The experimental stimulus was continuous noise with its intensity alternating up and down in 20-dB steps as a consequence of periodic (10 per second) modulation by a trapezoidal envelope (1.0 ms rise and fall times). The duration of the high-level phase was 40 ms, that of the low-level phase was 60 ms. The noise, with gaussian amplitude distribution, was generated by a General Radio random noise generator (Model 1390-B) and was shaped by a 1/3-octave equalizer to produce nearly flat (±2.5 dB) power spectral density of the acoustic output of the ER-2, over the range of 300 to 8000 Hz, as sensed by the ER-10 and analyzed by a Hewlett-Packard 3561A dynamic signal analyzer.

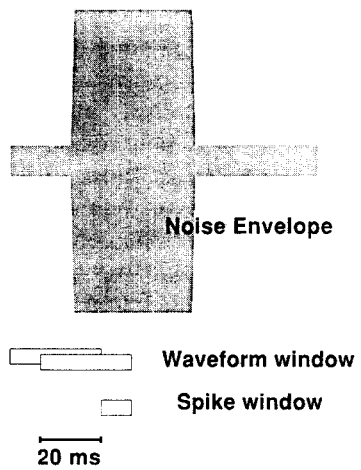

Fig. 1. Graphical depiction of stimulus presentation. A full stimulus cycle comprised 40 ms of high level noise, and 60 ms of low level noise. The duration of the waveform window used for analysis in each experiment was 30 ms. The duration of the spike window was varied from experiment to experiment, but fixed within a given experiment. During a given experiment, the trailing edge of the waveform window always occurred at the time of a spike and therefore could occur any time that the spike window was open. The two overlapping boxes show the range of waveform window positions for the spike window shown.

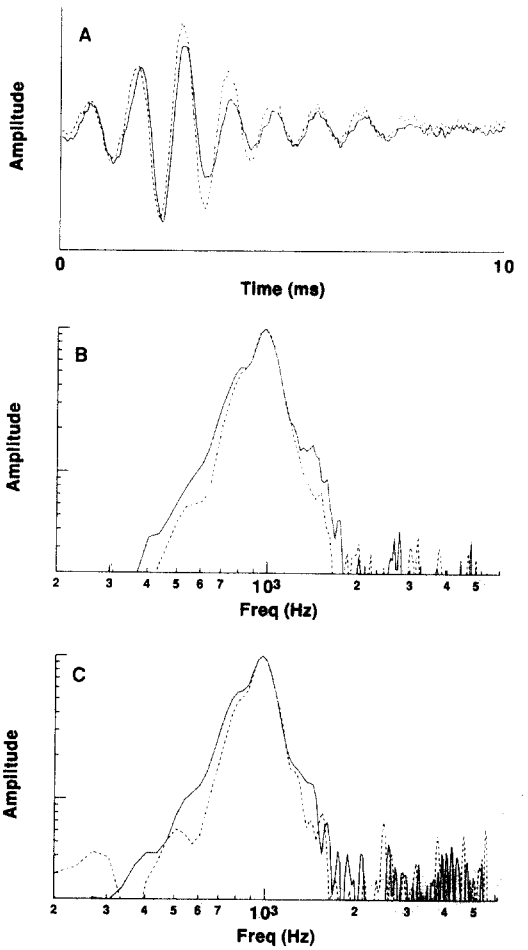

Fig. 2. REVCOR-derived responses of a unit (CF approximately 1 kHz) to low level noise (dashed line) and high level noise (solid line). 2A. REVCOR-derived impulse responses, normalized to show approximately the same peak amplitude. For the dotted line (averaged over 17,634 spikes), the spike window spanned all but the first 10 ms of the low level noise presentation of each stimulus cycle. For the solid line (18,952 spikes), the spike window spanned all but the first 10 ms of the high level noise. The short latency of the impulse response is typical of our results for units with low CFs and is puzzling inasmuch as the experimental and analytical setups (including the noise bandwidth) were identical to those for units with higher CFs, which showed longer latencies (e.g., Fig. 3A). 2B. Normalized discrete Fourier transform (DFT) amplitude functions for the waveforms in panel 2A. 2C. Normalized DFT amplitude functions for REVCOR-derived impulse responses for the same axon but with the spike window spanning the second 10 ms of the high level noise presentation (solid line, 6,406 spikes), and the second 10 ms of the low level noise presentation (dashed line, 3,987 spikes).

Reverse correlation (REVCOR) was carried out over selected segments of the noise envelope. This was accomplished with a REVCOR setup with a 29.7-ms time window applied to the noise stimulus and an adjustable time window applied to the spike train (see

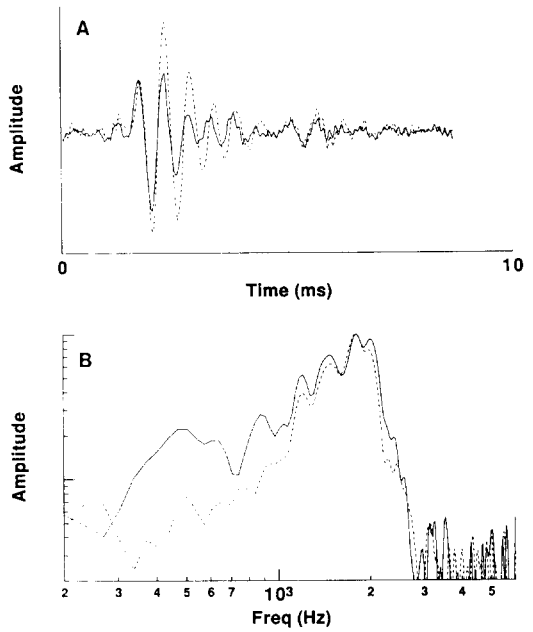

Fig. 3. Normalized REVCOR-derived impulse responses (3A) and their normalized DFT amplitude functions (3B) for a unit with a CF of approximately 1.8 kHz. During each stimulus cycle, the spike window for the solid line (averaged over 19,750 spikes) opened 5 ms after the onset of the high-level noise and spanned 35 ms, the spike window for the dashed line (averaged over 23,544 spikes) opened 8 ms after the onset of the low-level noise and spanned 52 ms.

Fig. 1). The noise-stimulus waveform was sampled and digitized. For each spike occurring during the time that the spike window was open, the digitized noise-stimulus waveform that occurred over the 29.7 ms immediately preceding the spike was saved. The digitized waveform was stored in 1024 time bins (yielding a time resolution of 29 μs per bin). REVCOR functions were obtained by taking the average value for each time bin over a large collection of such digitized waveforms, and then reversing the order of the bins. The position of the spike window relative to the amplitude-modulation envelope of the noise stimulus was adjustable. Thus, REVCOR functions (taken to be estimates of the cochlear-filter impulse response) not only could be derived separately for the high- and low-level phases of the noise stimulus, but also over any selected fraction of the high- or low-level phase. For each selection, the width and relative position of the spike window was fixed and the REVCOR sampling was carried out over many repetitions of the amplitude-modulation cycle.

3. Results

Fig. 2 shows results that are representative for the lower-CF axons in the study. In this case, the CF was between 940 and 1010 Hz. The high and low noise levels were 52 and 32 dB SPL (for 75 Hz bandwidth), respectively. After preliminary examination of the data, the nominal duration of the REVCOR-derived impulse response was taken to be 10 ms. Therefore, subsequent REVCOR analysis for this unit was begun at least 10 ms from the transition from one noise level to the other. Fig. 2A shows REVCOR-derived impulse responses taken over all but the first 10 ms of the high

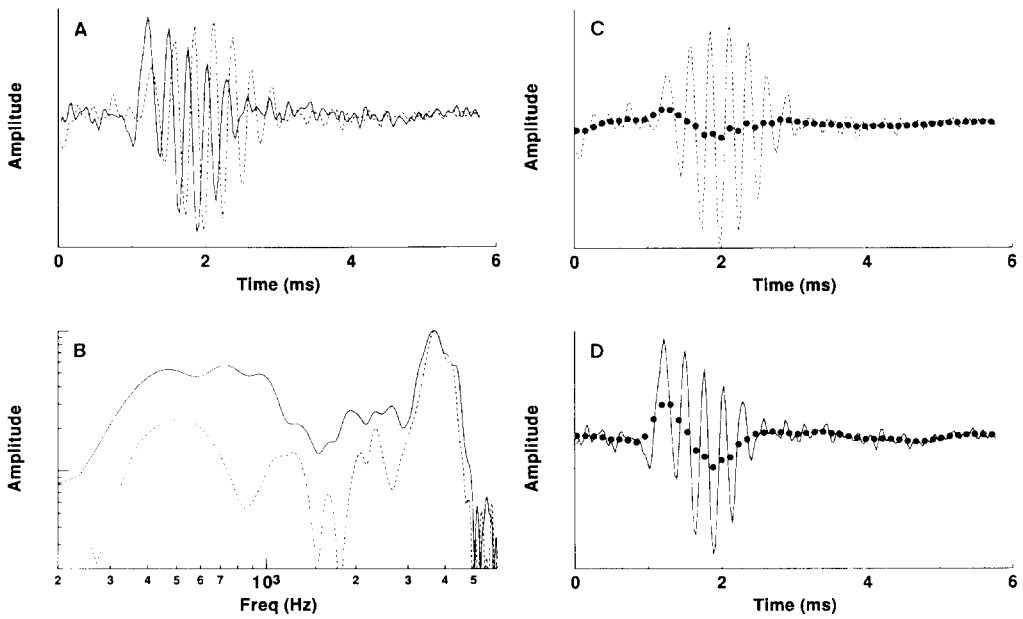

Fig. 4. Normalized REVCOR-derived impulse responses (4A, C and D) and their DFT amplitude functions (4B) normalized at the high-frequency peak (nominal CF) for a unit with a CF of approximately 3.7 kHz. As in Figs. 2 and 3, the response for high-level noise (averaged over 51,357 spikes) is shown with the solid line, that for the low-level noise (averaged over 61,400 spikes) with the dashed line. See text for description.

(solid line) and low (dashed line) level noise. Cycle-by-cycle examination reveals that the impulse response for the high-level noise is more heavily damped than that for the low-level noise. This difference is reflected in the bandwidths of the corresponding (normalized) DFT amplitude curves, shown in Fig. 2B. Each of the DFT amplitude curves in Fig. 2C were derived from REVCOR taken over a spike window 10 ms in duration and beginning 10 ms after the transition between noise levels. Clearly, during the second 10-ms segment of each phase of noise amplitude, the new tuning bandwidth already has been largely (if not completely) established. With the nominal duration of the impulse response being 10 ms, moving the leading edge of the spike wind closer than 10 ms from the noise-level transition would yield experimentally-induced distortion in the estimated impulse response. Thus, the changes seen in Fig. 2C have taken place in times (less than 10 ms) that are too short to be estimated by this method.

Fig. 3 shows REVCOR-derived impulse responses and their DFT amplitude curves for an axon with a CF between 1780 and 1850 Hz. The noise levels were 57 and 37 dB SPL (for 75-Hz bandwidth). In the DFT amplitude curve (solid line) for the higher noise level one can see a suggestion of the same sort of hump at low frequencies as that reported by Møller. We found that this feature consistently becomes more pronounced in axons with higher CFs. In Fig. 4, for example, the data were taken from an axon with CF between 3637 and 3738 Hz. The noise levels again were 57 and 37 dB SPL (for 75-Hz bandwidth). The impulse responses in Fig. 4A were derived for all but the first 7 ms of the high-level noise phase (solid line) and all but the first 7 ms of the low-level noise phase (dashed line). The corresponding DFT amplitude curves are shown in Fig. 4B. For the higher noise level, the relative amplitude of the low-frequency hump makes it quite conspicuous. The corresponding feature in the impulse response is illustrated in Figs. 4C and D. In each of these figures, short-term mean amplitudes of the impulse response are depicted as bold dots. These values were derived by twice applying a running 11-bin average (with uniform weights) to the impulse-response waveform. What emerges with the dots is an image of a heavily-damped, lower-frequency component (corresponding to the broad, low-frequency hump in Fig. 4B) summed with a more lightly damped, higher-frequency component (corresponding to the sharper, high-frequency peak in Fig. 4B).

Fig. 5A shows the DFT amplitude curves for the axon of Fig. 4, immediately before and after the transition from low- to high-level noise. The dashed curve was taken with a spike window spanning the last 4 ms of the low-level noise; the solid curve was taken with a spike window that opened 3 ms after the transition to

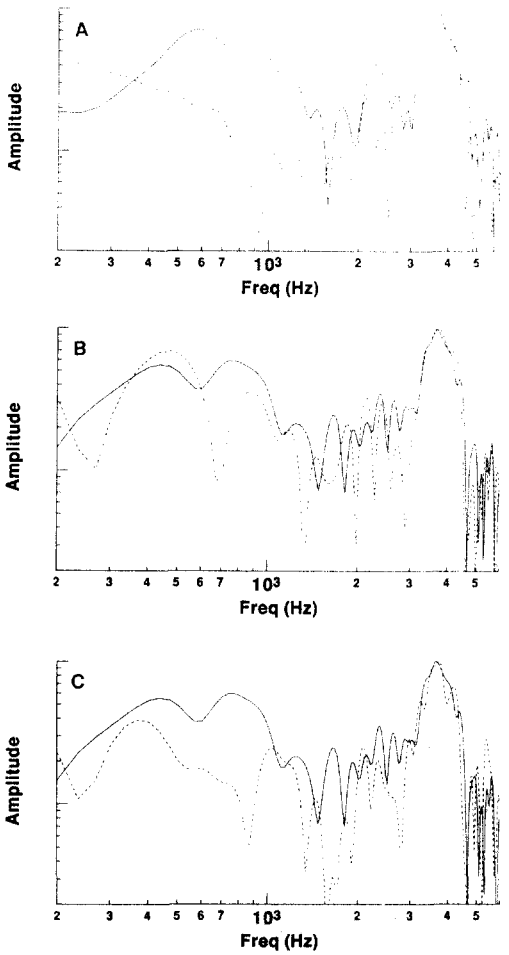

Fig. 5. Normalized DFT amplitude functions for REVCOR-derived impulse responses taken with variously-positioned, 4-ms spike windows for the axon of Fig. 4. Panel 5A compares the response at the end of the low-level noise (dashed line, 5,886 spikes) to the response at the beginning of the high-level noise (solid line, 8,288 spikes). 5B compares the response at the end of the high-level noise (solid line, 6,469 spikes) to the response at the beginning of the low-level noise (dashed line, 4,225 spikes). 5C compares the response at the end of the high-level noise (solid line, 6,469 spikes) to the response at the end of the first quarter of the low-level noise (dashed line, 5,435 spikes).

high level and remained open for 4 ms. In this case, 3 ms was taken to be the nominal duration of the REVCOR-derived impulse response. Clearly, the relative amplitude of the low-frequency hump and the broadening of the high-frequency peak both have occurred very quickly (evidently within the 3 ms nominal duration of the impulse response). For the transition from high level noise to low level, the paucity of spikes immediately after transition (commonly associated with adaptation in primary auditory afferents) decreases the signal to noise ratio in the REVCOR-derived functions taken with short-duration spike windows beginning close to the transition. Nevertheless, one often can see trends in the resulting waveforms. In Fig. 5B, for example, comparing the DFT amplitude curve for the

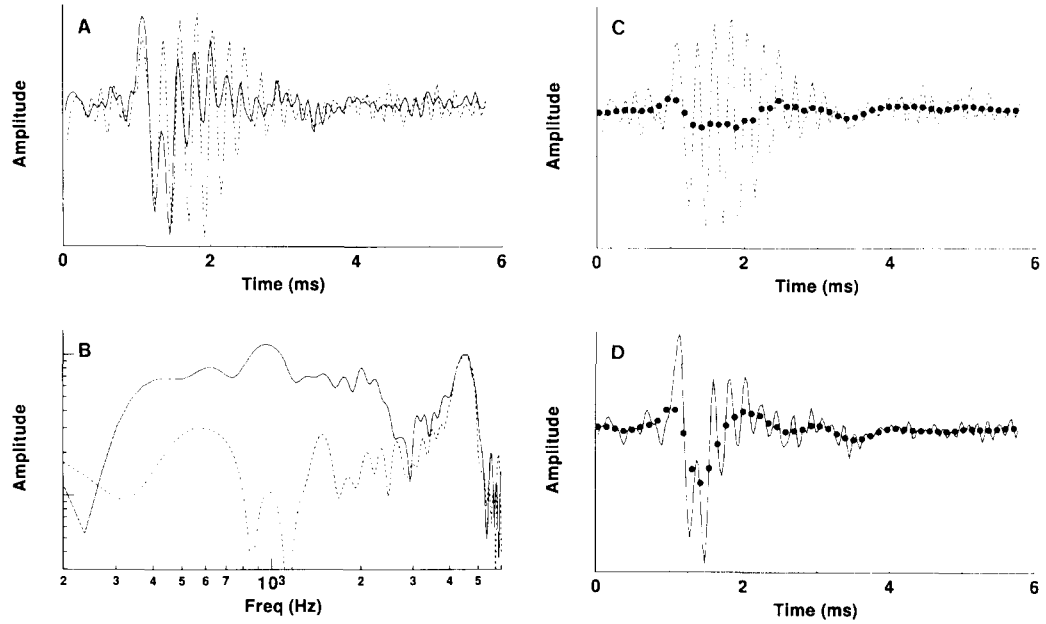

Fig. 6. Normalized REVCOR-derived impulse responses (6A,C and D) and DFTs (6B) to the high-level noise (solid line, 25,150 spikes) and low-level noise (dashed line, 23,405 spikes) of a 4.5 kHz CF unit. Note the heavily damped low frequency component (heavy dots) of the high level impulse response (6D), corresponding to the low frequency hump of the DFT (solid curve in 6B).

last 4 ms of the high-level noise (solid line) with that for a window of 4 ms duration, beginning 4 ms after the transition to low level (dashed line), one can see that the relative amplitude of the low-frequency hump and the bandwidth of the high-frequency peak have not changed much. Changes do begin to appear in a DFT amplitude curve for a window of 4 ms duration, beginning 11 ms after the transition to low level (Fig. 5C).

Fig. 6 shows results from an axon with CF between 4494 and 4562 Hz. The noise levels again were 57 and 37 dB SPL (for 75-Hz bandwidth). The heavily-damped, low-frequency component of the impulse response is especially obvious for the high-level stimulus in this case. In fact, the shapes of the impulse responses in Figs. 6A, 6C and 6D represent typical behavior among the higher-CF axons in this study. Fig. 7 shows the

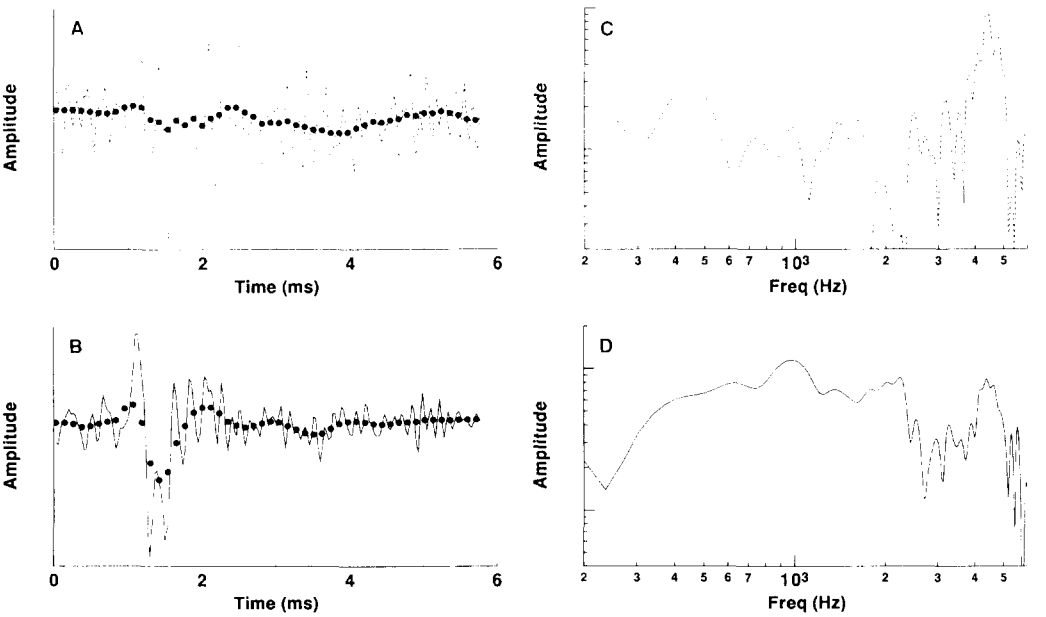

Fig. 7. Responses obtained with spike windows positioned close to the noise-window amplitude transitions for the unit of Fig. 6. Panels 7A and C show REVCOR-derived impulse response (averaged over 2,343 spikes) and its DFT amplitude, respectively, after the high-to-low level noise transition. Panels 7B and D show the responses (averaged over 8,103 spikes) obtained after the low-to-high level transition.

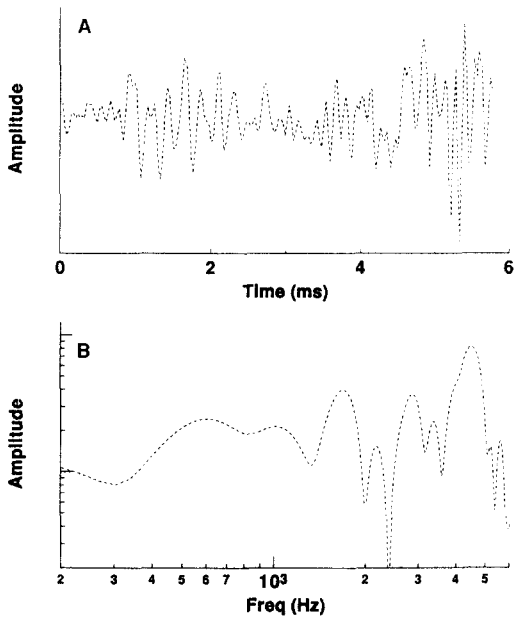

Fig. 8. Responses (averaged over 1,887 spikes) obtained for the unit of Fig. 6 with windows positioned even closer to the transition from high-to-low-level noise than illustrated in Fig. 7. Panel 8A shows the REVCOR-derived impulse response, and 8B shows the DFT amplitude obtained from that portion of the waveform of 8A that is free of the artifact produced by the transition.

REVCOR-derived responses for spike windows close to the noise-amplitude transitions. For the impulse response of Fig. 7A and the corresponding DFT amplitude curve of Fig. 7C, the spike window was 6 ms in duration and opened 7 ms after the transition from high- to low-level noise. Notice that the shapes of the impulse response and DFT amplitude curve already have reached those of Fig. 6 for low-level noise. For the impulse response and corresponding DFT amplitude curve of Figs. 7B and 7D, the spike window was 7 ms in duration and opened 3 ms after the transition from low- to high-level noise. The shapes already have reached those of Fig. 6 for high-level noise.

When a spike window comparable to that for the high-level noise response in Fig. 7 (i.e., a 7 ms window opening 3 ms after the transition) was used for the low-level noise, the proximity to high-level noise created an artifact in the impulse response. This can be seen beginning at 3 ms in Fig. 8A. To compensate for this problem, we carried out the DFT over only the first 3 ms of the waveform of Fig. 8A. The resulting amplitude curve, shown in Fig. 8B, suggest that the low-level tuning properties already are established (i.e., within 3 ms).

4. Discussion

With respect to the stimulus-intensity dependence of estimated cochlear impulse responses, the observations reported in this paper replicate, for the gerbil, those by Møller (1977, 1978, 1986) for the rat and those by Evans (1977) and Carney and Yin (1988) for the cat. All three species show increased damping of the estimated impulse response and corresponding broadening of its DFT. Our data seem to extend these results to a higher range of frequencies. In doing so, they show low-frequency humps (in the units with higher CFs) that are much more exaggerated than those reported previously (by Møller). Our data also show, for the first time, that the intensity-dependent changes in the impulse response take place very rapidly-- in both directions.

For each of the higher frequency units (i.e., CFs greater than approximately 2 kHz), the hump revealed by the higher-intensity noise could be taken to imply the presence of two filters, tuned to different frequencies and exhibiting markedly different dependence on stimulus level. The impulse responses of both filters seem to have properties (e.g., non-monotonic envelope, non-constant ringing frequency) that one would associate with high dynamic order (e.g., many eigenfrequencies) rather than simple resonances (Møller and Nilsson, 1979; Lewis et al., 1990). Dual filters have been implied previously by neural data, including data from otoacoustic emission experiments (e.g., see Brown and Williams, 1993). They also appear in several recent cochlear models (e.g., Allen and Fahey, 1993; Neely and Stover, 1993). The fact that our evidence for two filters is stronger at higher-intensity stimuli suggest that these filters are not the same as those implied by the otoacoustic emission data of Brown and Williams, where the effects of one member of the putative filter pair disappeared at higher stimulus levels.

The evidence observed by us and others for increased damping in response to increased stimulus level can be explained in various ways (e.g., see Marmarelis, 1991; Eggermont, 1993). Our purpose in carrying out this project, however, was to contribute to development of descriptive models of the behavior of the cochlea as a whole. We have not attempted to relate our observations to emergent properties of synthetic models of the cochlea (i.e., to models synthesized from descriptions of putative underlying mechanisms or models comprising various combinations of linear and non-linear processes). The rapidity with which tuning changed in response to rapid changes in stimulus intensity, however, should establish constraints on the classes of applicable synthetic models.

Acknowledgements

The research reported here was supported by the Deafness Research Foundation, the Office of Naval Research (Grant N00014–91-J-1333), and the National

Institute of Deafness and Communicative Disorders (Grant DC-00112). We thank Eva Hecht for help in preparing the illustrations.

References

Allen, J.B. and Fahey, P.F. (1993) Evidence for a second cochlear map. In: H. Duifhuis, J.W. Horst, P. van Dijk, S.M. van Netten (Eds.), Biophysics of Hair Cell Sensory Systems. World Scientific Press, London, pp. 296–303.

Brown, A.M. and Williams, D.M. (1993) A second filter in the cochlea. In: H. Duifhuis, J.W. Horst, P. van Dijk, S.M. van Netten (Eds.), Biophysics of Hair Cell Sensory Systems. World Scientific Press, London, pp. 72–77.

Carney, L.H. and Yin, T.C.T. (1988) Temporal coding of resonances by low-frequency auditory nerve fibers: single-fiber responses and a population model. J. Neurophysiol. 60, 653–1677.

de Boer, E. and de Jongh, H.R. (1978) On cochlear modeling: Potentialities and limitations of the reverse-correlation technique. J. Acoust. Soc. Am. 63, 115–135.

de Boer, E. and Kuyper, P. (1968) Triggered correlation. IEEE Trans BME 15, 115–135.

Eggermont, J.J. (1993) Wiener and Volterra analyses applied to the auditory system. Hear. Res. 66, 177–201.

Eggermont, J.J., Johannesma, P.I.M. and Aertsen, A.M.H.J. (1983) Reverse correlation methods in auditory research. Quart. Rev. Biophys. 16, 341–414.

Evans, E.F. (1977) Frequency selectivity at high signal levels of single units in cochlear nerve and nucleus. in E.F. Evans and J.P. Wilson (Eds.), Psychophysics and Physiology of Hearing. Academic Press, London, pp. 185–196.

Lewis, E.R. and Henry, K.R. (1989) Cochlear nerve responses to waveform singularities and envelope corners. Hear. Res. 39, 209–224.

Lewis, E.R., Yu, X. and Sneary, M. (1990) Further evidence for tuning mechanisms of high dynamic order in lower vertebrates. In P. Dallos, C.D. Geisler, J.W. Matthews, M.A. Ruggero and C.R. Steele (Eds.), Mechanics and Biophysics of Hearing. Springer-Verlag, New York, pp. 129–136.

Marmarelis, V.Z. (1991) Wiener analysis of nonlinear feedback in sensory systems. Ann. Biomed. Engrg. 19, 345–382.

Møller, A.R. (1977) Frequency selectivity of single auditory-nerve fibers in response to broadband noise stimuli. J. Acoust. Soc. Am. 62, 136–142.

Møller, A.R. (1978) Frequency selectivity of the peripheral auditory analyzer studied using broad band noise. Acta Physiol. Scand. 104, 24–32.

Møller, A.R. (1986) Systems identification using pseudorandom noise applied to a sensorineural system. Comp. Math. Appl. 12A, 803–814.

Møller, A.R. and Nilsson, H.G. (1979) Inner impulse response and basilar membrane modeling. Acustica 41, 258–262.

Neely, S.T. and Stover, L.J. (1993) Otoacoustic emissions from a nonlinear, active model of cochlear mechanics. In: H. Duifhuis, J.W. Horst, P. van Dijk, S.M. van Netten (Eds.), Biophysics of Hair Cell Sensory Systems, World Scientific Press, London, pp. 64–71.